Cancer Cell
Article

EZH2 Is Required for Germinal Center Formation and Somatic EZH2 Mutations Promote Lymphoid Transformation

Wendy Béguelin,[1] Relja Popovic,[4,11] Matt Teater,[1,2,11] Yanwen Jiang,[1,2] Karen L. Bunting,[1] Monica Rosen,[1] Hao Shen,[1] Shao Ning Yang,[1] Ling Wang,[1] Teresa Ezponda,[4] Eva Martinez-Garcia,[4] Haikuo Zhang,[5] Yupeng Zheng,[6] Sharad K. Verma,[7] Michael T. McCabe,[7] Heidi M. Ott,[7] Glenn S. Van Aller,[7] Ryan G. Kruger,[7] Yan Liu,[7] Charles F. McHugh,[7] David W. Scott,[8] Young Rock Chung,[9,10] Neil Kelleher,[6] Rita Shaknovich,[1] Caretha L. Creasy,[7] Randy D. Gascoyne,[8] Kwok-Kin Wong,[5] Leandro Cerchietti,[1,3] Ross L. Levine,[9,10] Omar Abdel-Wahab,[9,10] Jonathan D. Licht,[4,*] Olivier Elemento,[2,*] and Ari M. Melnick[1,3,*]

[1]Division of Hematology/Oncology, Department of Medicine
[2]Institute for Computational Biomedicine
[3]Department of Pharmacology
Weill Cornell Medical College, New York, NY 10021, USA
[4]Division of Hematology/Oncology, Robert H. Lurie Comprehensive Cancer Center, Feinberg School of Medicine, Northwestern University, Chicago, IL 60611, USA
[5]Department of Medical Oncology, Dana-Farber Cancer Institute, Boston, MA 02215, USA
[6]Departments of Chemistry and Molecular Biosciences, Chemistry of Life Processes Institute, Northwestern University, Evanston, IL 60208, USA
[7]Cancer Epigenetics Discovery Performance Unit, Cancer Research, Oncology R&D, GlaxoSmithKline, 1250 S. Collegeville Road, Collegeville, PA 19426, USA
[8]Centre for Lymphoid Cancer, Departments of Pathology and Experimental Therapeutics, British Columbia Cancer Agency, British Columbia Cancer Research Centre, Vancouver, BC V5Z 1L3, Canada
[9]Human Oncology and Pathogenesis Program
[10]Leukemia Service, Department of Medicine
Memorial Sloan-Kettering Cancer Center, New York, NY 10065, USA
[11]These authors contributed equally to this work
*Correspondence: j-licht@northwestern.edu (J.D.L.), ole2001@med.cornell.edu (O.E.), amm2014@med.cornell.edu (A.M.M.)
http://dx.doi.org/10.1016/j.ccr.2013.04.011

SUMMARY

The EZH2 histone methyltransferase is highly expressed in germinal center (GC) B cells and targeted by somatic mutations in B cell lymphomas. Here, we find that EZH2 deletion or pharmacologic inhibition suppresses GC formation and functions. EZH2 represses proliferation checkpoint genes and helps establish bivalent chromatin domains at key regulatory loci to transiently suppress GC B cell differentiation. Somatic mutations reinforce these physiological effects through enhanced silencing of EZH2 targets. Conditional expression of mutant EZH2 in mice induces GC hyperplasia and accelerated lymphomagenesis in cooperation with BCL2. GC B cell (GCB)-type diffuse large B cell lymphomas (DLBCLs) are mostly addicted to EZH2 but not the more differentiated activated B cell (ABC)-type DLBCLs, thus clarifying the therapeutic scope of EZH2 targeting.

INTRODUCTION

The majority of B cell lymphomas arise from germinal center (GC) B cells, which form part of the humoral immune response to T cell-dependent antigen stimulation (Ci et al., 2008; Klein and Dalla-Favera, 2008). GC B cells originate from mature, VDJ rearranged, antigen-naive B cells present in lymphoid follicles that, upon activation, migrate to the center of lymphoid follicles and

Significance

We show that EZH2 is required for the humoral immune response. EZH2 function is linked to de novo formation of bivalent chromatin domains at genes required for exit of B cells from the GC. Mutant EZH2 alleles tip the balance of these domains toward increased lysine 27 residue of histone 3 methylation, leading to more potent and permanent silencing. This manifests as differentiation blockade, GC hyperplasia, and accelerated lymphomagenesis in cooperation with BCL2. Wild-type and mutant EZH2 functions are essential for GCB-type DLBCLs but dispensable for ABC-DLBCLs. These data reveal the function of EZH2 and its mutants in mature B cells and lymphomas and provide the basis for specific rational combinatorial targeted therapy for GCB-type DLBCLs.

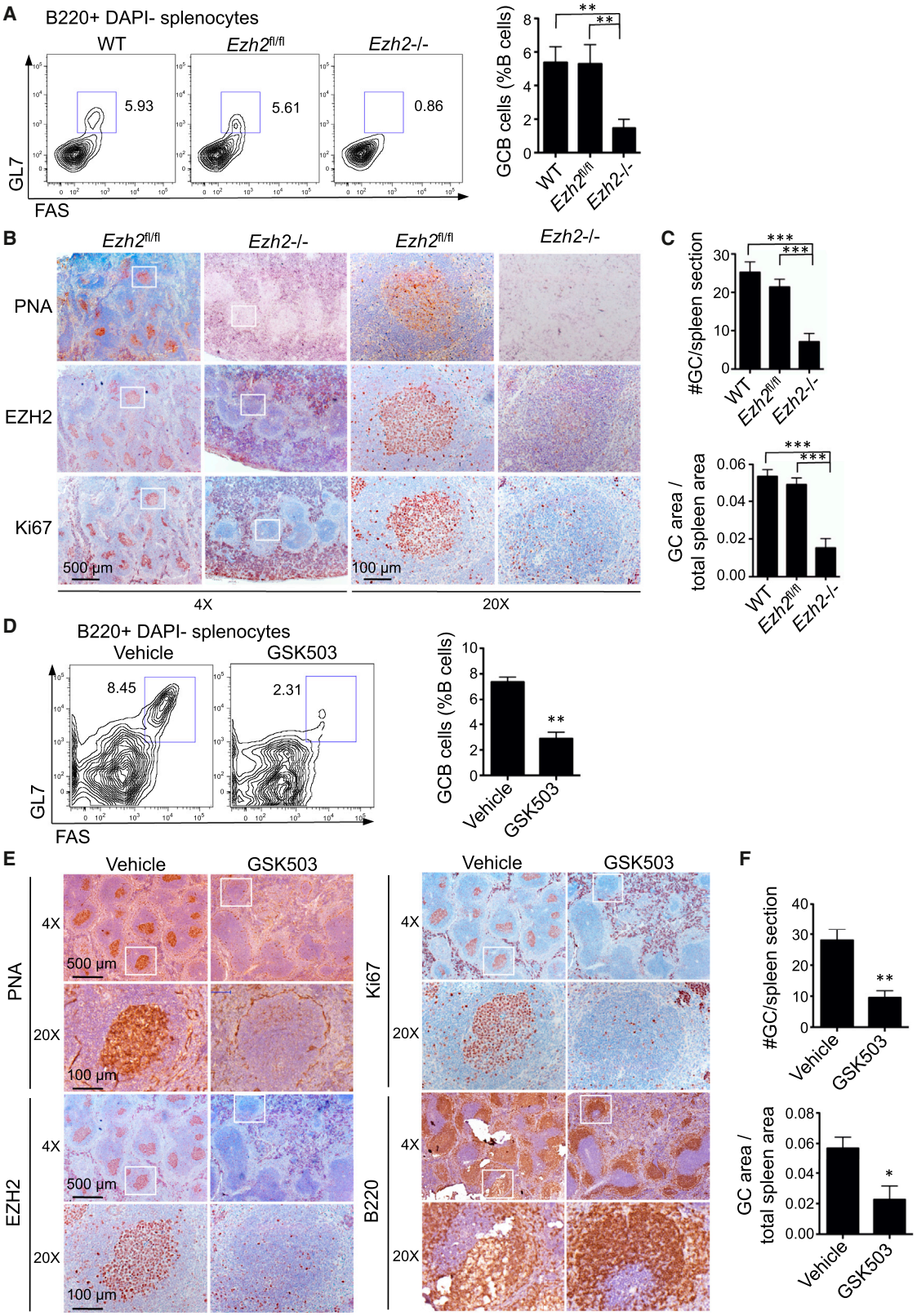

(legend on next page)

form GCs. GC B cells are unique in their ability to replicate at an accelerated rate while undergoing somatic hypermutation, which requires attenuation of DNA damage sensing and replication checkpoints. Clonal expansion of these cells is followed by terminal differentiation of the subset of B cells that encode high affinity antibodies; by contrast, the remainder of GC B cells undergoes apoptosis. The rapid proliferation of GC cells with concomitant attenuation of DNA damage responses increases the risk of oncogenic mutations as a byproduct of somatic hypermutation and class switch recombination. Such mutations can lead to the development of diffuse large B cell lymphoma (DLBCL) and follicular lymphoma (FL) (Alizadeh et al., 2000; Klein and Dalla-Favera, 2008). Understanding how B cells impose and maintain the GC phenotype may thus provide important clues that could explain the pathogenesis of GC B cell-derived lymphomas and inform the design of rational therapeutic strategies for patients with DLBCL and FL.

Upon activation, GC B cells upregulate and highly express EZH2, a SET domain containing histone methyltransferase that forms part of polycomb repressive complex-2 (PRC2) (Raaphorst et al., 2000; Velichutina et al., 2010). EZH2 catalyzes methylation of the lysine 27 residue of histone 3 (H3K27) but is mostly catalytically active when complexed with the PRC2 components EED and SUZ12 (Chase and Cross, 2011; Mahmoudi and Verrijzer, 2001). H3K27 methylation is a repressive histone mark associated with gene repression (Cao et al., 2002; Czermin et al., 2002; Müller et al., 2002). EZH2 is critical for normal development, and EZH2 knockout embryos fail to implant and undergo gastrulation (O'Carroll et al., 2001). EZH2 plays a major role in regulating gene expression patterning in embryonic and tissue-specific stem cells, where it contributes to setting genes into a "poised" bivalent state characterized by the simultaneous appearance of the H3K27me3 repressive mark along with the H3K4me3 activation-associated mark (Bernstein et al., 2006; Shin et al., 2012). These poised bivalent genes can then be resolved into activated or stably repressed loci, depending on lineage commitment. In tissue-specific stem cells, EZH2 and partner proteins are critical for the proper coordination of differentiation and proliferation. For example, conditional knockout studies in early stages of B cell differentiation showed that EZH2 is important for normal immunoglobulin VDJ recombination in pre-B cells (Su et al., 2003). However, after the pre-B cell stage, EZH2 expression declines and is not detectable in mature B cells located within lymphoid tissues until these cells enter the GC reaction (Su et al., 2003; van Galen et al., 2004; Velichutina et al., 2010). Once B cells exit the GC reaction, EZH2 is once again downregulated (Velichutina et al., 2010).

We previously found that EZH2 target genes in GC B cells only partially overlap with EZH2 targets in embryonic stem cells, suggesting that it has GC-specific functions (Velichutina et al., 2010). Moreover, PRC2 components, including EZH2, are often highly expressed in GC B cell-derived DLBCL (van Kemenade et al., 2001), suggesting that PRC2 functions may contribute to lineage-based proliferation of malignant B cells. RNA-sequencing studies recently identified heterozygous somatic point mutations targeting the EZH2 SET domain, most commonly affecting the Y641 residue of EZH2, in ~30% of GC B cell (GCB)-type DLBCL and 10% of FL (Morin et al., 2010). These mutations alter the enzymatic activity of EZH2, resulting in a protein that fails to recognize unmodified H3K27 and preferentially converts mono- or dimethylated H3K27 to the trimethylated state (Sneeringer et al., 2010; Yap et al., 2011). DLBCL cell lines harboring EZH2 point mutations display aberrant accumulation of H3K27me3 compared to wild type (WT)-EZH2 cells (McCabe et al., 2012a; Sneeringer et al., 2010). The importance of EZH2 in maintaining the growth of lymphoma cells was demonstrated in small interfering RNA knockdown experiments (Velichutina et al., 2010) and more recently through the development of highly specific and potent EZH2 small molecule inhibitors (Knutson et al., 2012; McCabe et al., 2012b; Qi et al., 2012). However, the role and requirement for EZH2 and its mutant alleles in the formation of GCs and pathogenesis of B cell lymphomas has not been explored, nor is its mechanism of transformation known beyond the association with global cellular abundance of H3K27me3. Here, we explore the function of normal and mutant EZH2 in mature B cells and lymphomas using murine models and human cells. We also address the mechanisms of action of WT and mutant EZH2 and provide the basis for rational, combinatorial, targeted therapy for GCB-type DLBCL.

RESULTS

EZH2 Is Required for Formation of Germinal Centers

The increased expression of EZH2 in GC B cells suggested that this protein plays critical roles in mediating the phenotype of GC B cells. However, EZH2 deletion is lethal in early embryonic development (O'Carroll et al., 2001), and its inducible knockout in early hematopoietic cells perturbs lymphoid differentiation at the pre-B cell stage (Su et al., 2003). We therefore crossed conditional *Ezh2*$^{-/-}$ mice with the Cγ1cre strain, which expresses cre recombinase in GC B cells (Casola et al., 2006). Upon reaching immunological maturity, *Ezh2*$^{fl/fl}$, *Ezh2*$^{-/-}$, and WT control mice were injected with T cell-dependent antigen sheep red blood cells (SRBC) to induce GC formation and sacrificed 10 days later, at which time the GC reaction is at its peak. EZH2 loss resulted in a marked reduction in the number of splenic GC (GL7^{+}/FAS^{+}/B220^{+}) B cells (Figure 1A). Immunohistochemical analysis using peanut agglutinin (a GC B cell marker) revealed a reduction in the number ($p < 0.0001$) and size ($p = 0.001$) of GCs in *Ezh2*$^{-/-}$ versus *Ezh2*$^{+/+}$ mice, whereas there was no change in GCs in *Ezh2*$^{fl/fl}$ mice (Figures 1B and 1C). There was also marked reduction in Ki67-positive cells consistent with loss of the proliferative GC B cell compartment (Figure 1B). The histologic appearance of the spleen and primary lymphoid

Figure 1. EZH2 Is Required for Germinal Center Formation

(A–C) EZH2$^{fl/fl}$, EZH2$^{-/-}$, and WT C57BL6 control mice (n = 5 per group) were immunized with SRBC to induce GC formation. (D–F) C57BL6 mice were immunized with SRBC and treated with GSK503 (150 mg/kg/day) or vehicle (n = 5 per group). (A and D) Representative flow cytometric plot of splenic GC cells and quantification. (B and E) Splenic tissue was stained with PNA, EZH2, Ki67, and B220. (C and F) Quantitative imaging of PNA staining from (B) and (E), respectively. Values in (A), (C), (D), and (F) are shown as mean ± SEM. t test, *$p < 0.05$, **$p < 0.01$, ***$p < 0.001$.

See also Figure S1 and Tables S1–S4.

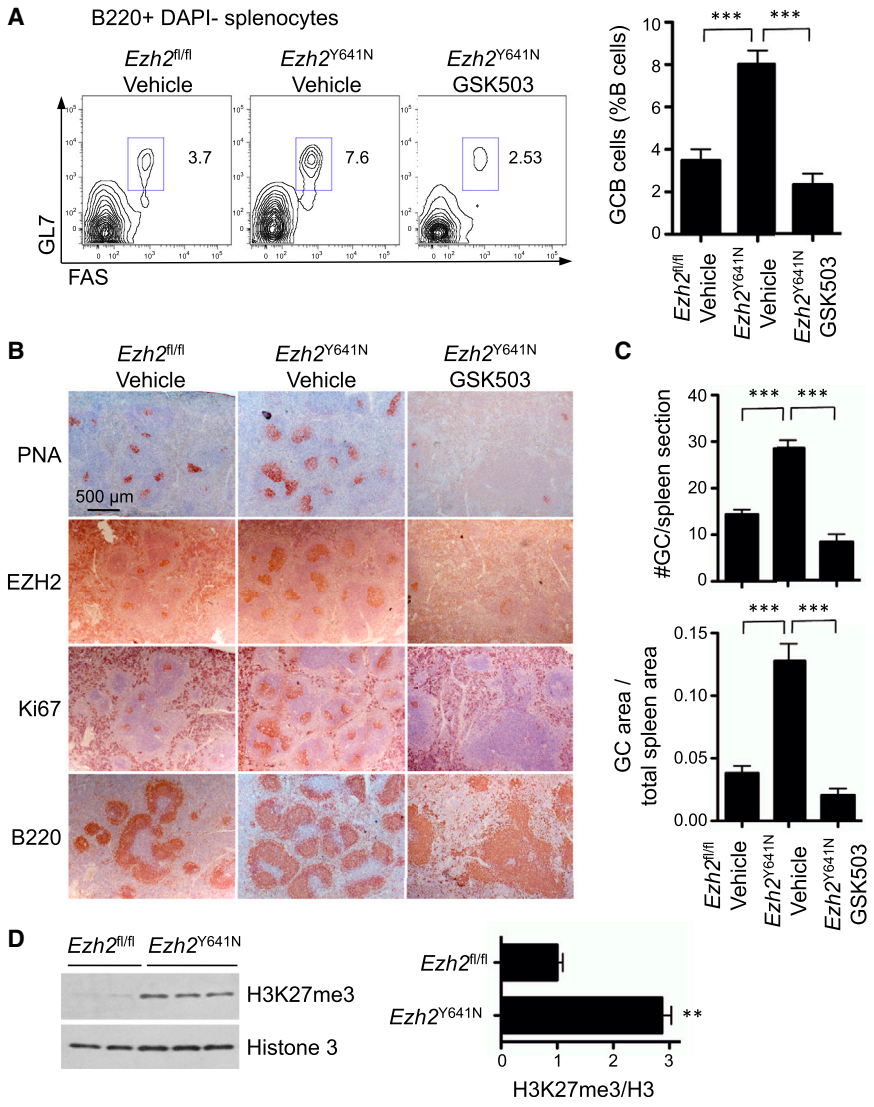

Figure 2. Mutant EZH2 Induces Germinal Center Hyperplasia

$EZH2^{fl/fl}$ and $EZH2^{Y641N}$ mice were immunized with NP-KLH and treated with GSK503 (150 mg/kg/day) or vehicle (n = 6 per group).

(A) Representative flow cytometric plot of splenic GC cells and quantification.

(B) Splenic tissue was stained with PNA, EZH2, Ki67, and B220.

(C) Quantitative imaging of PNA from (B).

(D) Immunoblotting from whole cell lysates from sorted splenic GC B cells ($GL7^+/FAS^+/B220^+$).

Values in (A), (C), and (D) are shown as mean ± SEM. t test, **p < 0.01, ***p < 0.001.

See also Figure S2.

follicles was otherwise normal (Figure S1A available online), and marginal zone and follicular B cells were unaffected (Figure S1B). The few residual GC B cells were EZH2 positive, consistent with incomplete cre-mediated excision of *Ezh2* and the notion that GC B cells require EZH2 (data not shown). A similar phenotype was observed when $Ezh2^{-/-}$ mice were injected with nitrophenyl-keyhole limpet hemocyanin (NP-KLH), which induces cognate high affinity antibodies (Figure S1C). The defect in GC formation was accompanied by impaired immunoglobulin affinity maturation with reduction in formation of high-affinity antibodies (Figure S1D).

We next immunized a cohort of C57BL6 mice with SRBC followed by once daily treatment with 150 mg/kg/day GSK503, a specific EZH2 methyltransferase inhibitor or vehicle. GSK503 was designed by performing high-throughput screening for EZH2 methyltransferase-inhibiting compounds followed by chemical optimization (Figure S1E). GSK503 inhibits the methyltransferase activity of WT and mutant EZH2 with similar potency (K_i^{app} = 3–27 nM) and is structurally related to GSK126 and GSK343 (McCabe et al., 2012b; Verma et al., 2012). GSK503 was >200-fold selective over EZH1 (K_i^{app} = 636 nM) and >4,000-fold selective over other histone methyltransferases (Tables S1–S4; Figures S1F and S1G). GSK503 displayed favorable pharmacokinetics in mice (Figures S1H and S1I) and was thus selected for use in in vivo experiments. We assessed the effects of GSK503-mediated EZH2 inhibition in vivo in GC B cells. GSK503 but not vehicle prevented the formation of GC after SRBC or NP-KLH immunization, phenocopying the *Ezh2* null phenotype. GSK503 treatment led to reduced numbers of GC B cells by flow cytometry, reduced number and volume of GCs by immunohistochemistry, and impaired formation of high-affinity antibodies (Figures 1D–1F, S1J, and S1K). There was no effect on marginal zone or follicular B cells (Figure S1L). Immunoblot analysis revealed that GSK503 reduced the level of H3K27me3 in splenocytes, confirming inhibition of the catalytic function of EZH2 in vivo (Figure S1M). Collectively, these data demonstrate that EZH2 is required for the formation of GCs and immunoglobulin affinity maturation and that this function is dependent on its histone methyltransferase activity.

Mutant EZH2 Induces Germinal Center Hyperplasia

Given that EZH2 was essential for development of GC B cells, we surmised that gain of function EZH2 mutants might reinforce these actions, with implications for lymphomagenesis. To address this point, we generated mice conditionally expressing the $Ezh2^{Y641N}$ lymphoma allele from the *ColA1* locus after excision of a lox-stop-lox cassette (Figures S2A–S2C). These animals were crossed into the Cγ1cre background to express $Ezh2^{Y641N}$ in GC B cells. Subsequent to immunization, these mice displayed greatly increased numbers of $GL7^+/FAS^+/B220^+$ GC B cells (p < 0.001; Figure 2A) and increased number and size of GCs (p < 0.0005; Figures 2B and 2C), while cre-negative $Ezh2^{fl/fl}$ animals showed no such effects. There was no effect on marginal zone or follicular B cell numbers or morphology

(Figure S2D). The phenotype was accompanied by a 3-fold increase in the abundance of H3K27me3 in sorted GC B cells from *Ezh2*^{Y641N} versus nonrecombined mice ($p < 0.005$; Figure 2D), analogous to what is observed in mutant EZH2 DLBCL cell lines (McCabe et al., 2012a; Sneeringer et al., 2010). Lymphoid GC hyperplasia was dependent on the increased histone methyltransferase activity as GSK503 treatment abrogated the *Ezh2*^{Y641N} GC hyperplasia phenotype ($p < 0.001$; Figures 2A–2C). These data demonstrate that Y641 mutation reinforces the GC phenotype-driving function of wild-type EZH2, resulting in an expansion of these proliferative and mutagenic cells. However, *Ezh2*^{Y641N} knockin mice did not develop B cell lymphomas (data not shown).

Mutant EZH2 Enhances Proliferation Effects in Part through Greater Repression of *CDKN1A*

To characterize in more detail the functions of EZH2 in mature B cells, we next expressed wild-type EZH2 and EZH2^{Y641} in murine BCL1 cells. BCL1 cells originate from a spontaneous murine lymphoproliferative disease, exhibit clonal somatic hypermutation, and have been used to model GC B cell biology (Blackman et al., 1986). BCL1 cells were transduced with GFP-expressing retrovirus harboring FLAG-tagged *Ezh2*^{Y641N}, *Ezh2*^{Y641F}, or WT *Ezh2* (Figure 3A). BCL1 cells transduced with EZH2^{Y641N} and EZH2^{Y641F} exhibited increased H3K27me3 levels, whereas H3K27me3 levels were unchanged by WT EZH2 (Figures 3A and 3B). EZH2^{Y641N} and EZH2^{Y641F} but not WT EZH2 conferred a significant growth advantage to BCL1 cells compared to vector infected cells ($p < 0.05$; Figure 3C). Moreover, EZH2^{Y641N} and EZH2^{Y641F} induced >10-fold expansion in colony formation as compared to WT EZH2 or vector (Figure 3D). Treatment with the specific EZH2 inhibitor GSK343 (Verma et al., 2012; Figures S1E–S1G) but not vehicle or the inactive chemical control GSK669 depleted H3K27me3 in BCL1 cells (Figure 3E) and abrogated colony formation induced by EZH2^{Y641N} or EZH2^{Y641F} (Figure 3F), confirming that enzymatic activity is required for their biological effects.

Given that BCL1 cells express endogenous EZH2 already (Figure 3A) and expression of exogenous EZH2 did not affect proliferation or colony formation in BCL1 cells, the effects we observed were specific to expression of mutant EZH2 in lymphoid cells. Recent studies have shown that EZH2 inhibitors and RNA interference suppress proliferation of EZH2 mutant DLBCL cells (Knutson et al., 2012; McCabe et al., 2012b; Qi et al., 2012; Velichutina et al., 2010). Consistent with these findings, small hairpin RNA (shRNA) depletion of EZH2 protein (Figure 3G) in EZH2 mutant Pfeiffer and WSU-DLCL2 cell lines led to >50% suppression of cell growth relative to shRNA control. shRNA-mediated depletion of EZH2 in WT EZH2 Farage cells led to a more modest and delayed 20%–40% decrease of growth (Figure 3H). GSK343 2 μM even more efficiently depleted H3K27me3 and more rapidly suppressed the growth of DLBCL cell lines, with greater effect observed in those with mutant EZH2 (Figures S3A and S3B). We identified *CDKN1A* as a direct EZH2 target in GC B cells and DLBCL (Velichutina et al., 2010; data not shown). Treatment of WT EZH2 cells with GSK343 led to a 2–4-fold induction of *CDKN1A*, while in mutant cell lines EZH2 inhibition led to 8–12-fold activation (Figure 3I). While EZH2 shRNA or GSK343 targeting of EZH2 led to a reduction in DLBCL cell viability, shRNA-mediated depletion of *CDKN1A* partially rescued this phenotype ($p < 0.05$; Figures 3J, 3K, and S3C). We performed gene expression profiling in diagnostic samples from patients with DLBCL and observed a trend for *CDKN1A* to be expressed at a lower level in GCB-DLBCL patients harboring EZH2 mutations versus GCB-DLBCL with wild-type EZH2 ($p = 0.07$; Figure S3D). These data are consistent with the notion that mutant EZH2 reinforces repression of GC B cell EZH2 target genes and that *CDKN1A* silencing may contribute, along with other genes, to the phenotypic effects of EZH2 in B cells.

EZH2 Mediates Differentiation Blockade in DLBCL Cells

GCB-DLBCLs exhibit differentiation blockade, locking them into the GC phenotype (Rui et al., 2011). Given that gain-of-function mutants induce an expansion in the population of GC B cells, we postulated that EZH2 might play a critical role in suppressing differentiation. We first compared RNA sequencing (RNA-seq) gene expression profiles in BCL1 cells transduced with WT or mutant EZH2. This analysis revealed that, in BCL1 cells, EZH2^{Y641N} or EZH2^{Y641F} increased repression of genes that are normally expressed upon terminal differentiation into plasma and memory cells when compared to EZH2-WT-expressing cells (gene set enrichment analysis [GSEA] false discovery rate [FDR] $q < 0.009$; Figure 4A). We induced differentiation in BCL1 cells using interleukin-2 (IL-2) and IL-5. These cytokines typically drive BCL1 cells toward a partial plasma cell phenotype accompanied by proliferation arrest (Blackman et al., 1986). Expression of EZH2^{Y641N} or EZH2^{Y641F} but not WT-EZH2 significantly impaired cytokine-induced proliferation arrest ($p < 0.05$; Figure 4B) and more profoundly suppressed activation of *Prdm1*, a key plasma cell differentiation gene ($p < 0.01$; Figure 4C).

Based on these data, we next examined whether EZH2 inhibition by GSK343 induces differentiation in human DLBCL cells. In GCB-type DLBCL cell lines (two mutant and one WT), EZH2 inhibitor treatment induced upregulation of the plasma cell proteins syndecan/CD138 and p63, upregulation of the memory cell marker CD27, and downregulation of the B cell surface marker CD20 (Figure S4A). Treatment with GSK343 but not GSK669 induced functional evidence of differentiation manifested by increased light chain and immunoglobulin production (Figure 4D) and morphologic changes consistent with plasma cell differentiation (Figure 4E). Gene expression analysis by quantitative PCR revealed upregulation of differentiation-related genes, including *PRDM1*, *IRF4*, and syndecan CD138 (Figure 4F), with greater effect generally noted in EZH2 mutant DLBCL cells ($p < 0.05$). Analysis of RNA-seq expression profiles induced by GSK343 in three DLBCL cell lines (two mutant and one WT EZH2) showed enrichment for transcriptional programs involved in plasma and memory B cell differentiation (FDR $q < 0.001$; Figure S4B). We also found strong enrichment in gene sets involved in exit from the GC reaction, including genes induced by CD40, interferon regulatory factor 4 (IRF4), IL10, and nuclear factor κB (NF-κB), and, notably, the activated B cell (ABC)-DLBCL signature (which consists of activation of these post-GC genes), as well as genes involved in apoptosis and immune responses (Figure 4G). Memory and plasma cell differentiation genes were among genes preferentially repressed in GCB-type DLBCL patients with EZH2 mutations as compared to GCB-DLBCL

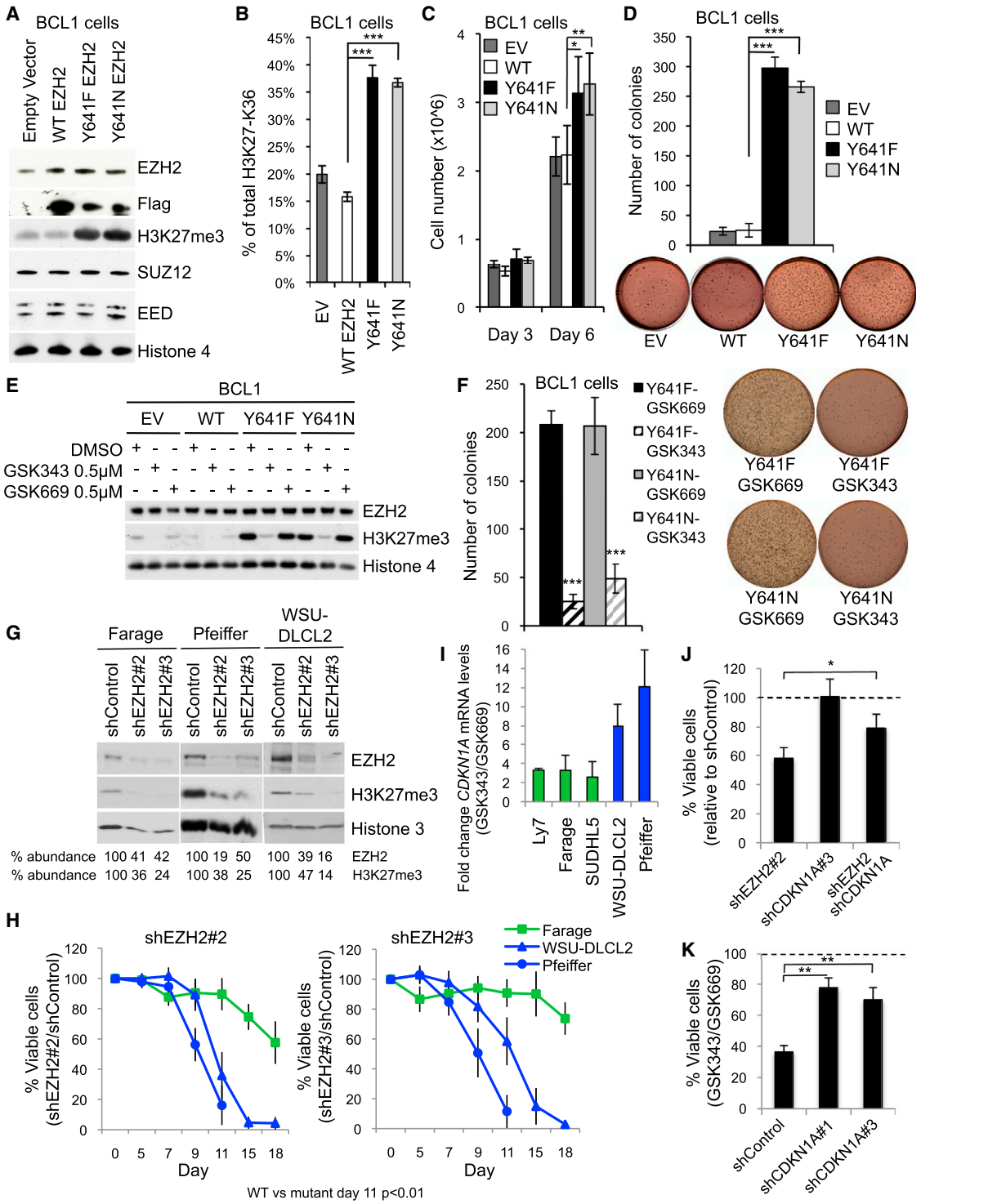

Figure 3. Mutant EZH2 Enhances Proliferation Effects through Repression of *CDKN1A*

(A) Immunoblotting from nuclear extracts from GFP+ BCL1 cells expressing GFP-FLAG-tagged EZH2^{Y641F}, EZH2^{Y641N}, or WT EZH2.

(B) Mass spectrometry measurement of H3K27me3 mark.

(C) Viability using trypan blue exclusion.

(D) Colony counts and representative pictures of transduced BCL1 cells.

(E) Immunoblotting was performed as in (A) with cells treated as indicated for 3 days.

(F) Colony counts and representative pictures of transduced BCL1 cells treated with 2.5 μM GSK669 or GSK343.

(G) Immunoblotting from whole cell lysates from yellow fluorescent protein (YFP)+ DLBCL cells expressing two independent EZH2 shRNAs or control.

(H) Viability of DLBCL YFP+ by flow cytometry using annexinV and DAPI exclusion. Green, WT EZH2; blue, mutant EZH2 cell lines.

(legend continued on next page)

patients with WT EZH2 (FDR q < 0.001; Figure 4H; Tables S5 and S6). *IRF4* was expressed at a significantly lower level in EZH2 mutant versus WT GCB-DLBCL patients (p = 0.01; Figure S4C). Collectively, these data suggest that EZH2 maintains the GC phenotype by suppressing transcriptional programs required for exiting the GC reaction and terminal differentiation. Mutant EZH2 augments these same functions by reinforcing repression of B cell differentiation genes.

Mutant EZH2 Aberrantly Represses Genes through Increased Promoter H3K27 Trimethylation

In order to gain insight into how mutant EZH2 might reinforce or alter normal EZH2-dependent transcriptional programs, we performed H3K27me3 chromatin immunoprecipitation sequencing (ChIP-seq) in BCL1 cells after transduction with $EZH2^{Y641N}$, $EZH2^{Y641F}$, WT EZH2, or vector and determined how gene expression in these cells responded to EZH2 inhibitors. Cells transduced with either $EZH2^{Y641N}$ or $EZH2^{Y641F}$ showed a marked increase in the abundance of H3K27me3 at gene promoters compared to EZH2 WT-transduced cells ($p < 2 \times 10^{-16}$ for both mutants; Figure 5A), and genes with abundant H3K27me3 were generally repressed ($p < 2 \times 10^{-16}$; data not shown). In addition, loci displaying increased H3K27me3 were more potently induced upon exposure of the BCL1-$EZH2^{Y641N}$/$EZH2^{Y641F}$ cells to GSK343 than EZH2 WT cells ($p < 5 \times 10^{-11}$ for $EZH2^{Y641N}$ and $EZH2^{Y641F}$; Figure 5B). Remarkably, those genes with increased H3K27me3 due to mutant EZH2 and more strongly induced by GSK343 corresponded to the set of human EZH2 target genes that acquire de novo H3K27me3 in human GC B cells (FDR q < 0.001; Figure 5C). Hence, mutant EZH2 appears to function at least in part by exaggerating the epigenetic silencing of normal GC B cell targets of wild-type EZH2.

EZH2 Is Linked to Formation of GC B Cell-Specific Bivalent Genes Involved in Differentiation

In stem cells, a subset of genes that are H3K27 trimethylated by EZH2 are also marked by the activating chromatin modification H3K4me3. These so-called "bivalent (H3K4me3/H3K27me3) domains" are believed to represent a mechanism for poising key lineage transcription factors so that they can be either activated or repressed during subsequent differentiation (Bernstein et al., 2006). We examined H3K27me3 and H3K4me3 distribution in purified primary human naive B (NB) cells and GC B cells by ChIP-seq. Notably, even though GC B cells are mature, committed cells (i.e., in contrast to stem cells), we find that they gain 1,026 new bivalent domains at promoters that are not found in NB cells (Figure 5D). Of these 910 (88%), bivalent promoters originate from H3K4me3-only promoters in NB cells (Figure 5D), indicating that most bivalent loci in GC B cells occur due to acquisition of H3K27me3, concordant with upregulation of EZH2 in these cells. ChIP-seq profiles from seven human GCB-DLBCL cell lines showed that these bivalent promoters were preferentially bound by EZH2 ($p < 1 \times 10^{-16}$; Figure 5E). In primary human GC B cells, bivalent genes were expressed at lower levels than loci with H3K4me3 alone but at higher levels than genes marked only by H3K27me3 ($p < 1 \times 10^{-300}$; Figure 5F). This is consistent with the proposed poised nature of bivalent genes in stem cells. GC B cell bivalent genes were highly enriched in gene sets associated with termination of the GC reaction, such as IRF4-induced, ABC-DLBCL, memory cell upregulated genes, as well as other GC B cell relevant genes, such as negative regulation of cell cycle (Figure S5A). The key regulatory transcription factors *IRF4* and *PRDM1* were among the GC B cell-specific bivalent genes, consistent with the notion that these genes are marked for dynamic activation upon exit from the GC reaction (Figure S5B) and that bivalent marks at this stage of B cell maturation function to transiently suppress terminal differentiation.

We wondered whether somatic mutation of EZH2 might lock these bivalent promoters into a more repressed configuration, perhaps helping to explain the irreversible differentiation blockade induced by mutant EZH2. Indeed, we observed that GC B cell bivalent genes were even more highly repressed in murine BCL1 cells transduced with $EZH2^{Y641N}$ and $EZH2^{Y641F}$ than in WT EZH2-transduced cells (FDR q < 0.001; Figure 5G). GC B cell bivalent domain genes were also significantly more repressed in human GCB-DLBCL patients with EZH2 somatic mutations compared to GCB-DLBCL with WT EZH2 (FDR q < 0.001; Wilcoxon p < 0.0006; Figures 5H and 5I). GC B cell bivalent genes involved in GC B cell differentiation, such as IRF4-induced genes, CD40-induced genes, and plasma/memory cell genes, were especially enriched among genes differentially expressed in mutant EZH2 DLBCL patients versus GCB-DLBCL specimens with wild-type EZH2 (Figures S5C and S5D). GC B cell bivalent genes were also significantly enriched among genes induced by GSK343 treatment of individual human DLBCL cell lines (FDR q < 0.001; Figure S5E; hypergeometric distribution test, $p = 3.4 \times 10^{-48}$). ChIP-seq showed enrichment of H3K27me3 at GCB bivalent genes in DLCBL cell lines ($p < 2 \times 10^{-16}$; data not shown). To confirm that bivalent marks are indeed occurring at the same chromatin regions within GC-derived DLBCL cells, we performed ChIP re-ChIP assays. The key regulatory transcription factors necessary for GC exit, *IRF4*, and *PRDM1*, as well as the proliferation checkpoint gene promoter *CDKN1B*, all shown to be putative GC B cell bivalent genes by our ChIP-seq experiments, were confirmed to be significantly co-occupied by H3K27me3 and H3K4me3 marks (Figure S5F). In contrast, *HOXA7* (which is silenced in mature B cells) was exclusively H3K27 trimethylated and *BCL6* (which is highly expressed in GC B cells) was almost exclusively H3K4 trimethylated. Collectively, these data suggest that, in normal GC B cell development, EZH2 reversibly suppresses terminal differentiation by forming or maintaining bivalent domains at specific loci that are also marked by H3K4me3, in addition to epigenetically silencing other genes through pure H3K27me3. In B cell

(I) qRT-PCR of *CDKN1A* in DLBCL cell lines treated with 2 μM GSK for 7 days. Green and blue code as in (H).
(J) Pfeiffer cells were cotransduced with the indicated shRNAs and viable YFP+ cells counted as in (H).
(K) Pfeiffer cells expressing two independent shCDKN1As or control were treated with 2 μM GSK for 6 days, and viability was measured as in (H).
Values in (B)–(D), (F), and (H)–(K) are mean of duplicate or triplicate ± SD. t test, *p < 0.05, **p < 0.01, ***p < 0.001. WT, WT EZH2.
See also Figure S3.

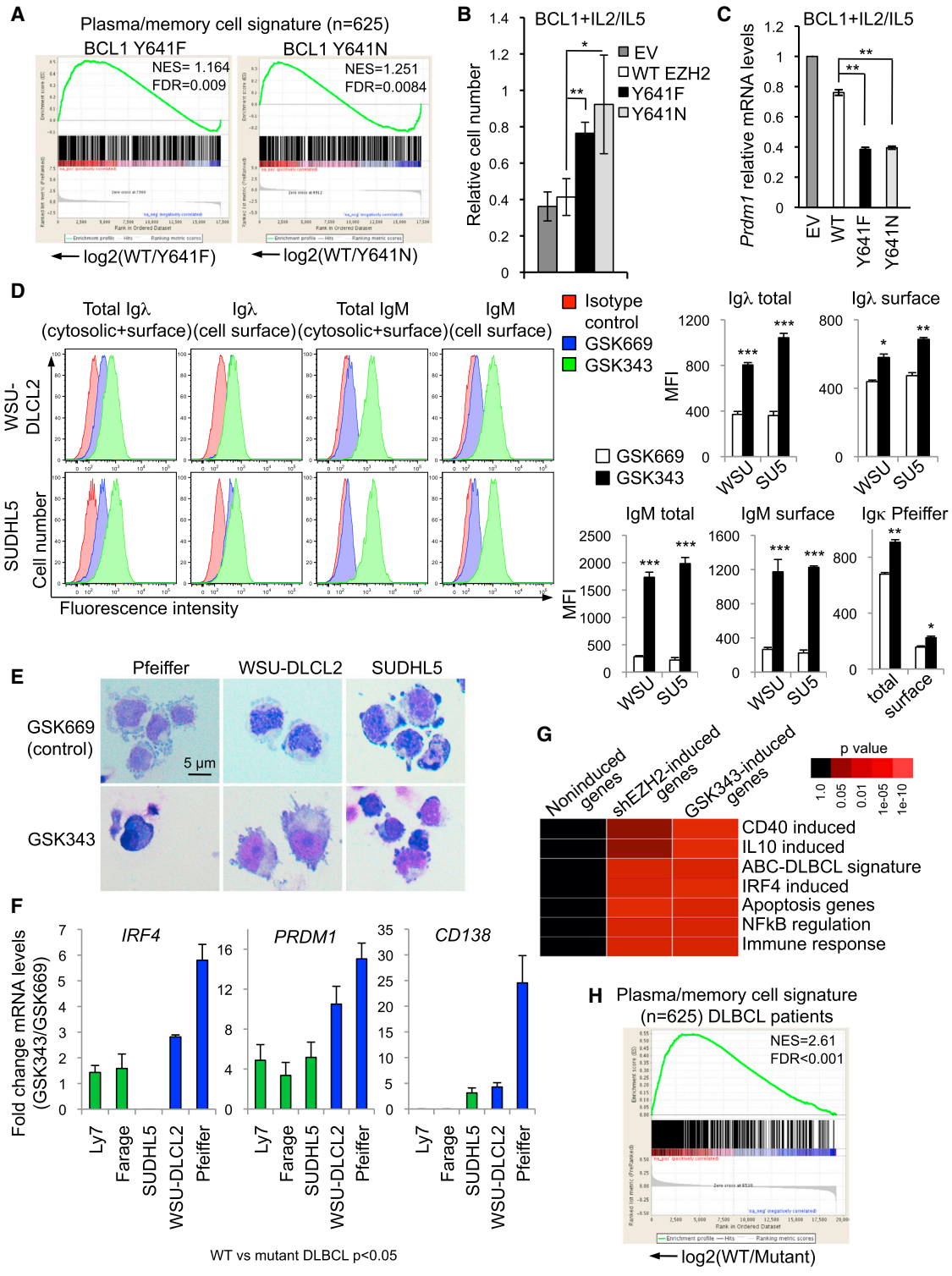

Figure 4. EZH2 Mediates Differentiation Blockade

(A) GSEA in WT versus mutant EZH2 BCL1-transduced cells. NES, normalized enrichment score.

(B) Cells were treated with 20 ng/ml IL2 and IL5 for 5 days and viability measured using trypan blue exclusion.

(C) qRT-PCR of *Prdm1*.

(D) Cells were treated with 2 μM GSK343 or control GSK669 for 7 days, and immunoglobulin (Ig) expression levels were examined by flow cytometry.

(E) Representative pictures of cells treated as in (D).

(F) qRT-PCR of indicated mRNAs in cells treated with 2 μM GSK for 7 days. Green, WT EZH2; blue, mutant EZH2 cell lines.

(legend continued on next page)

lymphomas, mutant EZH2 reinforces silencing of these genes, perhaps by increasing the frequency with which these genes are H3K27 methylated among tumor cells or by more subtle stoichiometric effects, tipping the balance of H3K27 toward trimethylation and away from demethylation.

EZH2 Cooperates with BCL2 to Generate Germinal Center-Derived Lymphomas

We next investigated whether mutant EZH2 might cooperate with other GC B cell lymphoma oncoproteins, such as BCL2, which is frequently translocated in patients with $EZH2^{Y641}$ mutations (Morin et al., 2011). We transduced bone marrow of vav-*Bcl2* mice with retrovirus expressing GFP and encoding WT EZH2, $EZH2^{Y641F}$, or GFP alone and transplanted them into lethally irradiated cohorts of ten recipients each (Figure 6A). Animals were immunized with SRBC every 4 weeks to ensure continuous formation of GCs. Macroscopic examination of spleens showed marked splenomegaly in $EZH2^{Y641F}$ versus EZH2 WT or empty vector (Figure 6B). Immunoblot analysis of splenic extracts showed similar levels of expression of EZH2 in the EZH2 WT and $EZH2^{Y641F}$ mice (Figure 6C). By contrast, H3K27me3 abundance was only elevated in splenocytes from $EZH2^{Y641F}$ mice, whereas H3K27me3 levels in EZH2 WT mice were similar to controls (Figure 6C). The livers of $EZH2^{Y641F}$ but not EZH2 WT mice were also significantly enlarged versus vector control (Figure 6D).

Detailed histopathologic examination and determination of clonality by immunoglobulin gene rearrangements indicated that, whereas 70% of $EZH2^{Y641F}$ mice developed a B cell lymphoma at 111 days, by contrast, only 20% of the WT EZH2 and none of the empty vector (EV) mice showed evidence of lymphoma at this time point. All EV and WT EZH2 mice displayed evidence of follicular hyperplasia, as expected in *Bcl2* transgenic mice (Figure 6E). However, examination of spleens in $EZH2^{Y641F}$/*Bcl2* mice revealed disruption of splenic architecture by neoplastic-appearing $B220^{+}$ B cells, most of which were EZH2 positive (Figures 6E and S6A). Neoplastic B cells were large (3 to 4 times the size of reactive lymphocytes) with pleomorphic nuclear morphology, fine chromatin and several nucleoli, ~60% Ki-67 expression, and were similar morphologically to human DLBCLs with centroblastic morphology (Figures S6A and S6B).

$EZH2^{Y641F}$/*Bcl2* mice displayed extensive infiltration of multiple tissues by neoplastic B cells, including lung, liver, lymph nodes, thymus, pericardiac soft tissue, pancreas, kidneys, salivary glands, urinary bladder, thyroid, ovarian bursa, bone marrow, skeletal muscles, small intestine, and stomach (Figures S6C and S6D; data not shown). Histologic examination of lungs revealed marked perivascular and peribronchiolar and mild interstitial infiltration of neoplastic B cells (Figure S6C). In the liver, infiltration was also extensive, with large periportal and to lesser extent perivenular and canalicular infiltrates (Figure S6D). Lymph nodes in $EZH2^{Y641F}$/*Bcl2* mice were also infiltrated by neoplastic cells with effacement of normal architecture and a mixture of nodular and diffuse patterns (data not shown). PCR amplification of IgVH regions from purified B220+ splenocytes revealed a dominant band in the background of few very weak bands, suggestive of a mostly monoclonal population of B cells (Figure 6F). Overall, the histopathological analysis was consistent with an aggressive DLBCL-like disease.

The two EZH2 WT animals that developed lymphoid malignancy included one with T cell and one with B cell disease and manifested a more indolent phenotype, including better preservation of the lymphoid architecture, minimal tissue infiltration in lung and liver, and were composed of plasma cells and reactive-appearing small lymphocytes (data not shown). A second cohort of *Bcl2*-transduced mice ($EZH2^{Y641F}$ n = 12, WT EZH2 n = 8, and GFP alone n = 9) were observed for survival. $EZH2^{Y641F}$/*Bcl2* manifested an accelerated lethal phenotype, with deaths due to progressive lymphoma beginning at day 90, whereas WT and EV mice began to die at day 140 (Figure S6E). The $EZH2^{Y641F}$ mice displayed a trend toward reduced median survival (median survival $EZH2^{Y641F}$: 203 days, WT EZH2: 252, EV: 243).

Finally, given that BCL2 and EZH2 can cooperate in lymphomagenesis, we hypothesized that BH3 mimetic drugs, such as obatoclax and ABT737, which block BCL2 function, might enhance the activity of EZH2 inhibitors. We exposed a panel of GCB DLBCL cells to increasing concentrations of GSK343 or GSK503, in combination with ABT737 or Obatoclax. In almost every cell line tested, the concentration of GSK343 or GSK503 required to yield 50% growth inhibition was reduced when cells were concomitantly treated with BH3 mimetics (Figures 6G and S6F). In order to determine the impact of EZH2 inhibitor combinatorial therapy in a preclinical model, we evaluated the action of GSK503 and Obatoclax alone or in combination in mice bearing human DLBCL cell line (SUDHL4 and SUDHL6) xenografts. Although both GSK503 and Obatoclax inhibited tumor growth alone, the combination of these inhibitors again more potently and significantly suppressed tumor xenograft growth (Figures 6H and S6G). EZH2 mutants therefore enable, accelerate, and maintain malignant transformation of GC B cells in cooperation with BCL2.

EZH2 Targeted Therapy Preferentially Affects GCB but Not ABC DLBCL Cells

EZH2 gain-of-function somatic mutations are restricted to GCB-type DLBCLs (Morin et al., 2010). Moreover, whereas EZH2 is a critical mediator of the GC B cell phenotype, which is reflected by the phenotype of GCB-DLBCL, it also represses genes and pathways that drive the phenotype of ABC-DLBCLs (e.g., *IRF4* and NF-κB pathway genes). We questioned whether these GCB-specific functions would translate to a specific role for EZH2 in the pathogenesis and therapeutic targeting of GCB versus ABC subtypes of DLBCL. Along these lines, we noted that EZH2 target genes were significantly more repressed in

(G) Heat map of overrepresented gene categories among genes upregulated by *EZH2* shRNA or 2 μM GSK343 for 7 days in Ly7, Ly1, SUDHL5, Farage, WSU-DLCL2, and Pfeiffer cells. Enrichment measured using hypergeometric p values.
(H) GSEA in GCB-DLBCL patient samples with WT versus mutant EZH2. Values in (B)–(D) and (F) are mean of duplicate or triplicate ± SD. t test, *$p < 0.05$, **$p < 0.01$, ***$p < 0.001$.
See also Figure S4 and Tables S5 and S6.

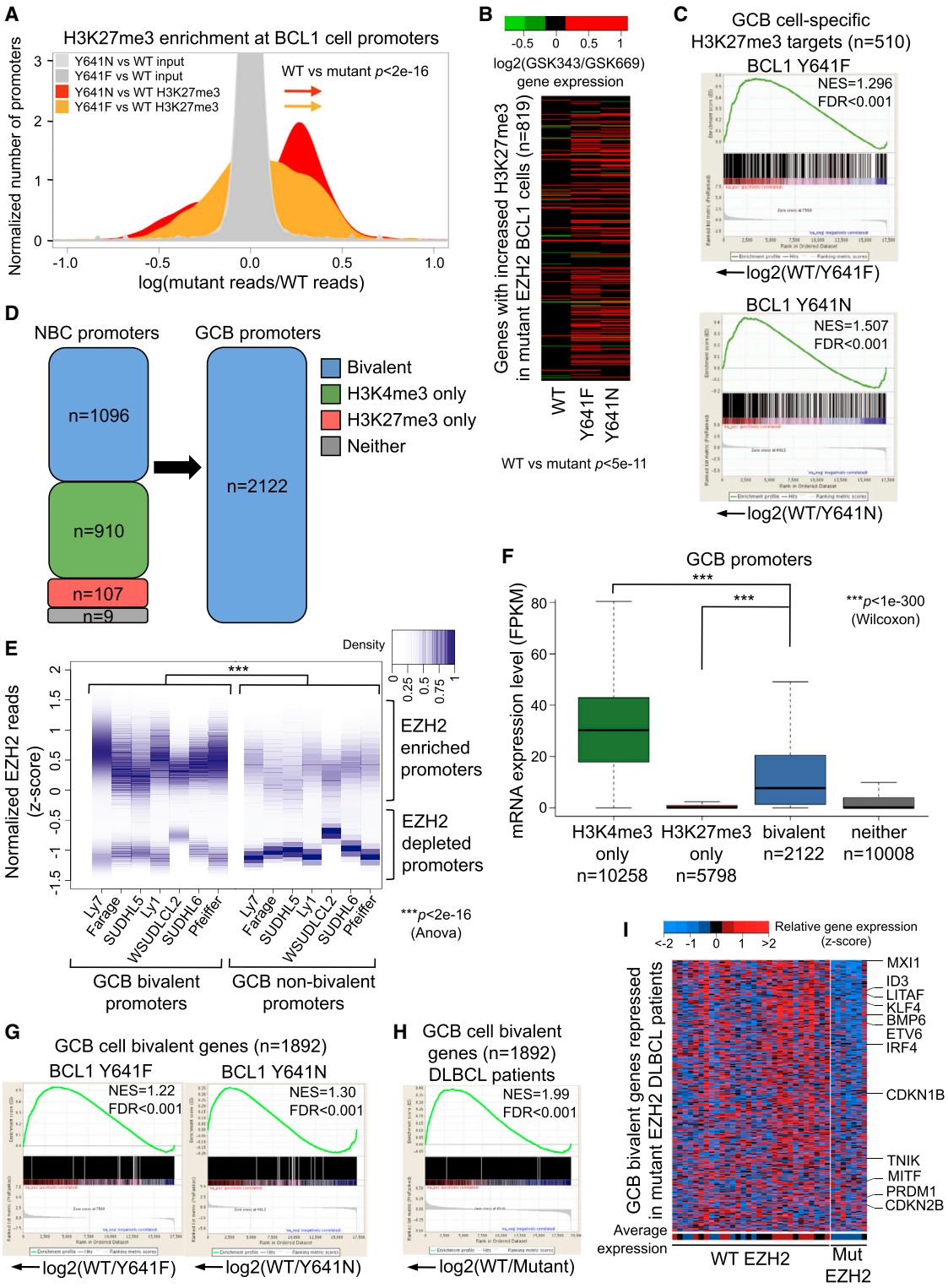

Figure 5. Mutant EZH2 Aberrantly Represses Genes by Increasing H3K27me3 at Promoters, and EZH2 Generates GC B Cell-Specific Bivalent Genes Involved in Differentiation

(A) ChIP-seq density plot.

(B) Heat map of change in expression of genes with increased H3K27me3 within promoters in BCL1 cells treated with 0.5 μM GSK for 3 days.

(C) GSEA of GCB cell-specific H3K27me3 targets in WT versus mutant EZH2 BCL1 cells.

(D) State of GCB cell bivalent promoters within naive B cells (NBC).

(E) Density strip representations of normalized EZH2 ChIP-seq reads within DLBCL cell line promoters.

(legend continued on next page)

GCB than in ABC DLBCLs, although even more significantly repressed when comparing ABC versus mutant EZH2 DLBCLs (Figure 7A). Gene set enrichment analysis revealed that EZH2 target genes (Figures 7B and 7C), including GCB bivalent genes (Figure S7A) were overrepresented among genes upregulated in ABC versus GCB DLBCLs (FDR q < 0.001), with enrichment scores even higher when comparing ABC versus mutant EZH2 DLBCLs (Figure S7A). Hence, EZH2 target genes, including those with bivalent marks at the GC stage of development, are expressed at relatively higher levels in ABC DLBCL cells, suggesting that EZH2 does not play a key role in their regulation in this form of lymphoma associated with the transformation of a postgerminal center B cell.

If EZH2 is not critical for the suppression of bivalent genes that drive proliferation once a cell exits the GC, then the biological effects of EZH2 inhibition would be predicted to be significantly different for ABC versus GCB lymphoma cells and ABC cells might be predicted to be relatively insensitive to EZH2 inhibitors. Therefore, we treated a panel of ABC and GCB DLBCL cell lines with increasing concentrations of GSK343 or GSK503. Strikingly, the drug concentrations required to inhibit 50% of growth (GI_{50}) for GCB lymphoma cell lines were in the 0.5–20 μM range, while, for ABC cells, no significant inhibition of cell growth was observed ($p = 0.0004$; Figures 7D and S7B–S7D). Exposure of EZH2 WT GCB cells to a fixed dose of 10 μM GSK343 or GSK503 led to 30%–75% reduction in viable cell number, while EZH2 mutant GCB cells were inhibited 50%–99%, suggesting a trend toward increased sensitivity. By contrast, this dose of drug led to no killing of ABC lymphoma cells ($p = 0.0001$ versus GCB; Figures 7E and S7E). EZH2 inhibitors completely demethylated H3K27me3 in ABC-DLBCL cells, indicating that resistance is biological and not due to failure of the drug to inhibit its target (Figure S7F). Collectively, these data suggest that EZH2 inhibitors may be useful for GCB DLBCL either with or without EZH2 mutations but are likely to be ineffective for ABC-type DLBCL.

DISCUSSION

In this manuscript, we show that EZH2 is a master regulator of the GC B cell phenotype, a function that is aberrantly reinforced by mutant EZH2 lymphoma disease alleles (Figure 7F). We find that EZH2 mediates its effects in GC B cells by repressing target genes involved in proliferation checkpoints (e.g., *CDKN1A*) and exit from the GC and terminal differentiation (e.g., *IRF4* and *PRDM1*). For immunoglobulin affinity maturation to occur, GC B cells must maintain their phenotype long enough to transit repeated rounds of division and somatic hypermutation. Hence, in the absence of EZH2 function, which is needed to support the GC B cell phenotype, mice display defective immunoglobulin affinity maturation. Normally, EZH2 levels decrease as B cells exit the GC reaction, enabling expression of genes that mediate terminal differentiation (Velichutina et al., 2010). However, in the presence of somatically mutated EZH2, suppression of GC exit genes and checkpoints persists, resulting in hyperplasia, and the presence of other oncogenic hits enables transformation to GCB-type DLBCL (Figure 7F). An alternative route leading to GCB-DLBCL could involve overexpression or aberrant maintenance of WT EZH2. Indeed, the highest quartile WT EZH2-expressing GCB-DLBCLs display a trend toward increased repression of EZH2 targets and tend to cluster together with EZH2 mutant patients (Figure S7G). The role of EZH2 in lymphomas is in large part to maintain or exaggerate (i.e., to hijack) the same EZH2 transcriptional program that is also required for development of normal GCs and immunoglobulin affinity maturation. Hence, GC B cells exhibit both oncogene and nononcogene addiction to EZH2.

The actions of EZH2 appear linked in part to de novo formation of bivalent chromatin domains, whereby genes marked by H3K4me3 in naive follicular B cells acquire H3K27me3 in GC B cells, concordant with upregulation of EZH2. In stem cells, bivalent (H3K4me3/H3K27me3) domains are hypothesized to maintain genes in a repressed but poised conformation, which can be subsequently dynamically activated or repressed according to lineage-specific differentiation programs (Bernstein et al., 2006; Shin et al., 2012). GC B cells represent a potentially unique situation where bivalent chromatin marks at specific genes are gained during differentiation, while in ES and tissue stem cell differentiation, they are lost. We however cannot exclude that other cell types and tumors that may overexpress EZH2 might also form bivalent domains at promoters. GC bivalent promoters are enriched in key gene sets involved in exit from the GC, such as IRF4- and CD40-induced genes, and genes upregulated in memory and plasma cells. As long as EZH2 maintains H3K27me3 at these loci, these genes are expressed at low levels, maintaining the GC phenotype. Repression of these genes is terminated as B cells exit the GC reaction and are selected for terminal differentiation. By contrast, EZH2 mutants disrupt the equilibrium of bivalent domains, enabling aberrant, persistent epigenetic silencing of genes, which in turn allows the GC B cell phenotype to persist, facilitating lymphoid transformation. Consistent with this hypothesis, we found that bivalent domain genes are the most aberrantly repressed in loci in EZH2 mutant DLBCL patient specimens. These data, along with the recent identification of frequent loss-of-function mutations in the histone methyltransferase protein MLL2 in B cell lymphomas (Lohr et al., 2012; Morin et al., 2011), suggest that the balance of H3K4me3 and H3K27me3 is disrupted and represents a therapeutic target in lymphoid malignancies. Mutations in MLL2 and EZH2 in lymphoma are not mutually exclusive (Morin et al., 2011), suggesting these mutations may cooperate to deregulate bivalent domains in GC B cells or that they also have independent roles in lymphomagenesis.

EZH2 mutants may also mediate their actions through additional mechanisms. We and others have noted that H3K27 ChIP-seq profiles as well as gene expression profiles induced by EZH2 inhibitors are variable between cell lines (McCabe et al., 2012b), suggesting that hyperactive EZH2 molecule might lead to epigenetic instability and stochastic aberrant epigenetic

(F) Boxplot of gene expression level of bivalent, H3K4me3 monovalent, H3K27me3 monovalent, and promoters not exhibiting either of these marks in GCB cells. (G and H) GSEA of GCB cell-specific bivalent genes in (G) WT versus mutant EZH2 BCL1 cells and (H) GCB-DLBCL patient samples with WT versus mutant EZH2. (I) Heat map of relative expression of GCB cell bivalent genes repressed in WT and mutant EZH2 GCB-DLBCL patient samples.
See also Figure S5.

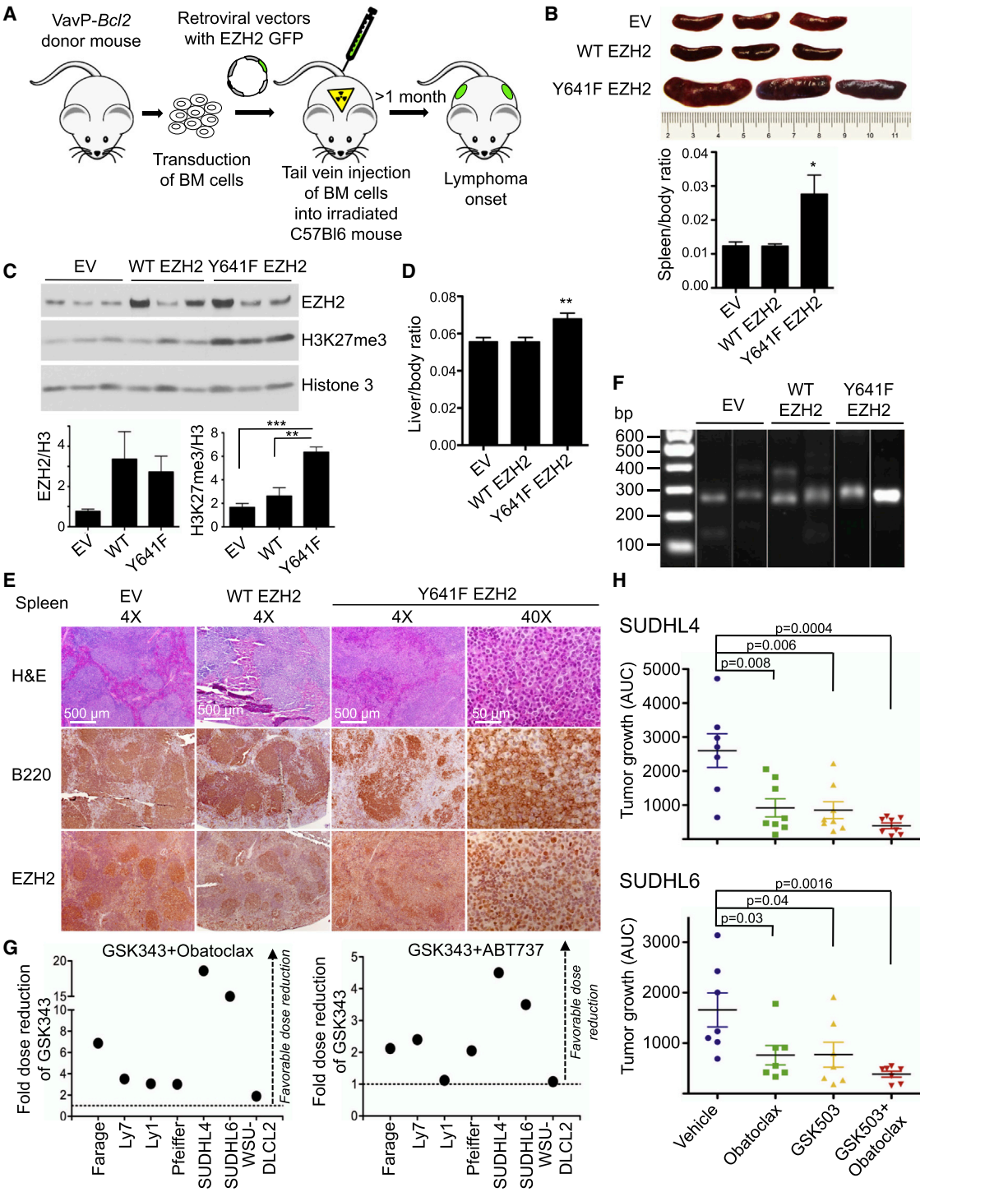

Figure 6. EZH2 Cooperates with BCL2 to Generate Germinal Center-Derived Lymphomas

(A) Bone marrow transplantation was performed using VavP-*Bcl2* transgenic donor mice.

(B) Representative pictures of spleens from mice sacrificed 111 days after transplantation and quantification of the spleen weight (n = 10 per group).

(C) Immunoblotting from whole cell lysates from splenocytes of transplanted mice.

(D) Quantification of the liver weight of transplanted mice (n = 10 per group).

(E) Splenic tissue from transplanted mice was stained with hematoxylin and eosin (H&E), B220, and EZH2.

(F) Tumor clonality analysis by RT-PCR performed in B220+ sorted splenocytes. Sample lanes separated by thin white lines were run on the same gel but were noncontiguous.

(G) Dose reduction plot for Obatoclax and ABT737 at GI_{90} after exposure of cells to increasing concentrations of GSK343 for 6 days. Data represent mean of triplicate experiments.

(legend continued on next page)

silencing of different gene sets. On the other hand, variability may be due to the fact that cell lines are genetically quite diverse and, under the stress of continuous passage in vitro, tend to drift apart epigenetically. This has been demonstrated in the case of cytosine methylation profiles, which differ considerably between lymphoma cell lines and primary lymphoma specimens (De et al., 2013). By contrast, primary human DLBCL specimens with mutant EZH2 showed a robust signature, consisting of greater repression of EZH2 target genes, including bivalent domains and with similarity to the EZH2 mutant signature induced in the isogenic BCL1 experimental model. Moreover, analysis of individual DLBCL cell lines after exposure to GSK343 showed upregulation of GC B cell EZH2 targets, including bivalent genes as well as phenotypic effects consistent with derepression of GC B cell EZH2 target genes. Notably, these studies underline that EZH2-mediated epigenetic effects are reversible in lymphomas, which is consistent with data in the prostate cancer field also showing that suppression of EZH2 can result in reactivation of genes with tumor-suppressing activity (Taniguchi et al., 2012; Yu et al., 2007).

Expression of mutant EZH2 alone in GC B cells was insufficient to induce development of DLBCL. In this way, EZH2 mutation appears analogous to many of the somatic mutations in acute myeloid leukemia (AML), which induce a myeloproliferative phenotype when expressed in murine hematopoietic stem cells but, when expressed together, cooperate to form AML (Shih et al., 2012). Mutant EZH2 induces a lymphoproliferative phenotype with expansion of the proliferative GC B cell compartment. Constitutive expression of the GC B cell oncoproteins BCL6 and BCL2 also manifest GC hyperplasia and a partially penetrant GC B cell lymphoma phenotype (Cattoretti et al., 2005; Egle et al., 2004). Hence, even though normal GC B cells exhibit features of partially transformed cells, such as suppression of proliferative checkpoints and attenuated DNA damage response, multiple oncogenic hits are still required for overt lymphomagenesis. This concept is supported by mutational profiling studies, revealing multiple concurrent somatic mutations in DLBCL specimens (Lohr et al., 2012; Morin et al., 2011), as well as our transplantation studies, demonstrating cooperation between mutant EZH2 and BCL2 in accelerating lymphomagenesis in mice. Knowledge of the genetic composition of lymphomas and how these cooperate to transform B cells affords the opportunity to rationally design combinatorial therapies. The enhanced antilymphoma activities of GSK343 and GSK503 in combination with anti-BCL2 therapies support this notion and point toward design of clinical trials geared toward the underlying biology of DLBCL and a reduced reliance on relatively nonspecific cytotoxic chemotherapy.

While previous reports have focused on the role of EZH2 inhibitors against mutant-EZH2 DLBCL (Knutson et al., 2012; McCabe et al., 2012b; Qi et al., 2012), our data indicate that EZH2 is a relevant target beyond those tumors. We find that GCB-type DLBCLs are dependent on wild-type EZH2 for their proliferation and survival, regardless of somatic mutation, although response to EZH2 inhibitors is slightly delayed as compared to mutant EZH2 DLBCL cells. This finding is in agreement with the absolute requirement of normal GC B cells for EZH2 and indicates that EZH2 is a lineage factor to which GC-type DLBCLs are addicted (Figure 7F). By contrast, ABC-DLBCLs do not require EZH2 to maintain their proliferation and survival. Indeed, the target genes repressed by EZH2 consist of many of same genes that define the ABC-DLBCL subtype. These data provide a mechanism by which increased EZH2-mediated repression of target genes can impair B cell differentiation and demonstrate that therapeutic targeting of EZH2 in GCB DLBCLs can induce differentiation and abrogate proliferation of GCB-DLBCLs with mutant or wild-type EZH2. We thus provide the basis for the expanded clinical translation of EZH2 inhibitors for the treatment of GCB-type DLBCLs. Clinical studies with pharmacologic EZH2 inhibitors will determine if this approach can improve outcomes for lymphoma patients. Although many GCB-type DLBCLs can be cured with combination chemoimmunotherapy regimens, these involve the use of toxic drugs that carry a lifelong risk of developing second malignancies. The current standard therapy for B cell lymphomas (RCHOP) wipes out the entire bone marrow of patients, and the B cell lineage is completely eradicated for months by rituximab (anti-CD20 antibody). In comparison, the transient suppression of high-affinity antibody formation by EZH2 inhibitors seems less likely to be clinically significant. By targeting the oncoproteins that drive and define the GCB DLBCL phenotype, it may be possible to reduce our reliance on cytotoxic drugs to eradicate this disease.

EXPERIMENTAL PROCEDURES

A more detailed description of the experimental procedures and reagents used in this study can be found in the Supplemental Experimental Procedures.

Generation of Conditional *Ezh2Y641N* Knockin Mice

Ezh2Y641N mice were generated by Frt-mediated targeting of *Ezh2Y641N* into the *ColA1* locus. The strategy for FLPe-mediated recombination (shown in Figure S2) was done as described previously (Beard et al., 2006). Briefly, homologous recombination was used to place an frt-hygro-pA cassette downstream of the *ColA1* locus. *Ezh2Y641N* complementary DNA (cDNA) was then targeted to the modified locus by coelectroporation of a pgkATGfrt vector carrying *Ezh2Y641N* and an FLPe transient expression vector. This pgkATGfrt contains the PGK promoter, an ATG initiation codon, an frt site, and a CAG promoter, driving the expression of *Ezh2Y641N*. Interspersed between the CAG promoter and *Ezh2Y641N* cDNA is a lox-stop-lox (LSL) cassette, ensuring that *Ezh2Y641N* is only expressed in the presence of cre-mediated excision of the LSL cassette. Interstrand intrachromosomal recombination at the frt sites results in loss of the PGKneopA cassette and insertion of *Ezh2Y641N* and pgkATG cassette to restore and confer hygromycin resistance. The integration site is located ~500 bp downstream of the 3′ UTR of the *ColA1* locus. This left the coding portion and 3′ UTR transcriptional control region of the *ColA1* gene intact. V6.5 ES cells were electroporated with this homologous targeting construct, and stable G418 clones were derived.

(H) Area under the curve (AUC) of the tumor growth curves for 20 days in SUDHL4 and SUDHL6 xenografted mice treated with vehicle (n = 7), Obatoclax (2 mg/kg/day, n = 8 in SUDHL4 and n = 7 in SUDHL6), GSK503 (150 mg/kg/day, n = 8 in SUDHL4 and n = 7 in SUDHL6), or the combination of Obatoclax and GSK503 (n = 8 in SUDHL4 and n = 7 in SUDHL6).

The p values were calculated by t test. Values in (B)–(D) and (H) are mean ± SEM. t test, *$p < 0.05$, **$p < 0.01$, ***$p < 0.001$. BM, bone marrow.

See also Figure S6.

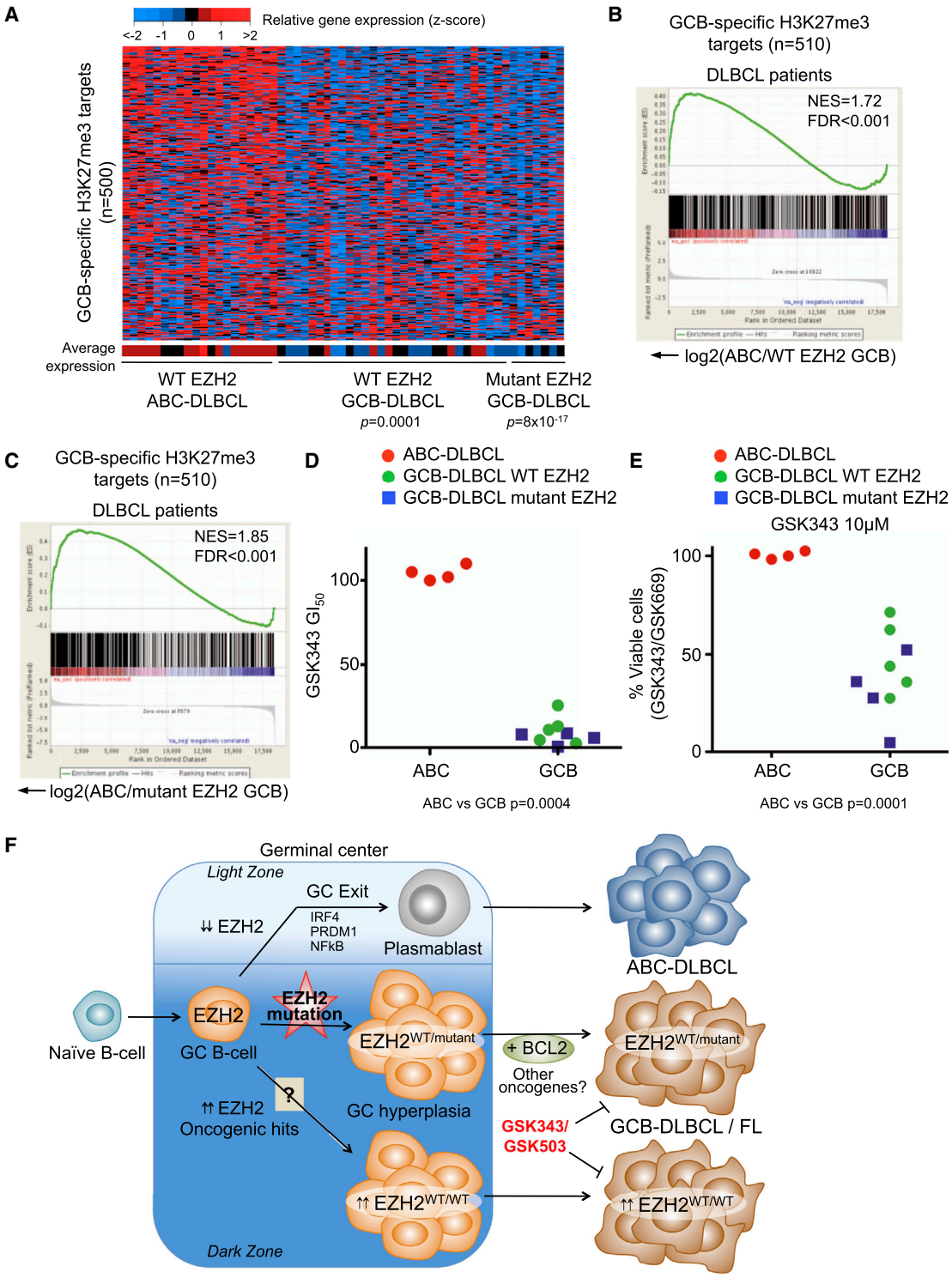

Figure 7. EZH2 Targeted Therapy Preferentially Affects GCB but Not ABC DLBCL Cells

(A) Heat map of relative expression of GCB-specific H3K27me3 target genes repressed in mutant EZH2 GCB-DLBCL patient samples.

(B and C) GSEA in ABC-DLBCL versus WT EZH2 GCB-DLBCL (B) and mutant EZH2 GCB-DLBCL (C).

(D and E) Four ABC-DLBCL (HBL-1, Ly3, U2932, and TMD8) and nine GCB-DLBCL cell lines (five WT EZH2: Ly7, Ly19, Farage, Ly18, SUDHL5 and four mutant EZH2: Pfeiffer, WSU-DLCL2, SUDHL4, SUDHL6) were exposed to increasing concentrations of GSK343 and GSK669 for 6 days. (D) GI_{50} of GSK343 relative to GSK669. (E) Cell viability at 10 μM GSK. Data are mean with 95% confidence interval for duplicate.

(F) When naive B cells are activated, EZH2 expression is highly induced. EZH2 is required for GC formation and Ig affinity maturation. EZH2 levels decrease as B cells exit the GC reaction, enabling expression of genes that mediate terminal differentiation (e.g., *IRF4, PRDM1,* and *NF-κB*). B cells in this "exiting" phase, such

(legend continued on next page)

Conditional Transgenic Murine Models

The Research Animal Resource Center of the Weill Cornell Medical College approved all mouse procedures. Conditional *Ezh2* knockout mice (*loxP*-flanked EZH2 allele, EZH2fl/fl) were a generous gift of Dr. Alexander Tarakhovsky, The Rockefeller University (Su et al., 2003). By crossing *Ezh2*fl/fl with the transgenic Cγ1cre strain (The Jackson Laboratory, 010611), we generated heterozygous mice, which were crossed to yield $Ezh2^{-/-}$ mice. As control group, we used *Ezh2*fl/fl Cγ1cre-negative littermates. $Ezh2^{Y641N}$ transgenic mice were crossed with Cγ1cre strain. The Cγ1cre-negative littermates were used as control group. Conditional *Ezh2* knockout and $Ezh2^{Y641N}$ knockin mice were used for assessment of the germinal center formation, which were induced with SRBC or NP-KLH.

DLBCL Patient Samples

Patient-deidentified leftover tissues were obtained at diagnosis from 69 patients with de novo DLBCL in Vancouver at the British Columbia Cancer Agency. Cases were selected on the basis of the presence of at least 80% of the neoplastic cells within the tumor section. The use of human tissue was approved by the research ethics board of the Vancouver Cancer Center/University of British Columbia and the Weill Cornell Medical Center. For additional information, see Table S6 and Supplemental Experimental Procedures.

ChIP-seq and mRNA-seq Library Preparation and Illumina Sequencing Processing

ChIP-seq and RNA-seq libraries were prepared using the Illumina ChIP-Seq and TruSeq RNA sample kits, respectively, according to the manufacturer. Libraries were validated using the Agilent Technologies 2100 Bioanalyzer and Quant-iT dsDNA HS Assay (Life Technologies) and 8–10 pM sequenced on HiSeq2000 sequencer as follows: ChIP-seq, 1 × 50 and messenger RNA sequencing (mRNA-seq), 2 × 50. RNA-seq data were aligned to transcripts using TopHat (Trapnell et al., 2009), gene expression quantified in fragments per kilobase of exon per million fragments mapped (Mortazavi et al., 2008), and differentially expressed genes identified. ChIP-seq experiments from human B cells, human cell lines, and murine cells were aligned to the hg18, hg19, and mm9 genome, respectively, using ELAND. H3K4me3 ChIP-seq reads were called into peaks using the ChIPseeqer framework ($p < 10^{-15}$ and fold-change threshold 2) (Giannopoulou and Elemento, 2011), and H3K27me3 and EZH2 ChIP-seq reads were quantified in 1 kb bins genome-wide, identifying regions of enrichment as consecutive bins with read counts greater than 1 SD of the genome-wide mean. Data analysis is described in Supplemental Experimental Procedures.

ACCESSION NUMBERS

The Gene Expression Omnibus accession numbers for the ChIP-seq, RNA-seq, and the expression microarray data reported in this paper are GSE45982 and GSE23501.

SUPPLEMENTAL INFORMATION

Supplemental Information includes seven figures, six tables, and Supplemental Experimental Procedures and can be found with this article online at http://dx.doi.org/10.1016/j.ccr.2013.04.011.

ACKNOWLEDGMENTS

We thank Dr. Alexander Tarakhovsky (Rockefeller University) for sharing the EZH2 conditional knockout mouse strain. A.M.M. is supported by the Burroughs Wellcome Foundation and Chemotherapy Foundation. A.M.M., R.L.L., and J.D.L. are supported by the Samuel Waxman Cancer Research Foundation and a collaborative transnetwork grant from the National Cancer Institute Physical Sciences in Oncology Center program (U54 CA143869 and CA143879). J.D.L., A.M.M., and O.E. are supported by a Leukemia and Lymphoma Society Specialized Center of Research Excellence, and A.M.M. and J.D.L. are supported by the T & C Schwartz Family Foundation. O.A.-W. is an American Society of Hematology Basic Research Fellow and is supported by a grant from the NIH K08 Clinical Investigator Award (1K08CA160647-01). L.C. is a Raymond and Beverly Sackler Scholar and Scholar of the American Society of Hematology. D.W.S. is supported by a CIHR postdoctoral fellowship award, and R.D.G. is supported by a New Frontiers in Cancer Terry Fox Program project grant (No. 019001). O.E. and A.M.M. are supported by NCI R01 CA104348. O.E. is supported by the NSF CAREER grant and grants from the Starr Cancer Consortium. This work was enabled by the Beverly and Raymond Sackler Center for Physical and Biomedical Sciences as well as the Weill Cornell Epigenomics Core Facility. S.K.V., M.T.M., H.M.O., G.S.V.A., R.G.K., Y.L., C.F.M., and C.L.C. are employees of GlaxoSmithKline.

Received: January 13, 2013
Revised: March 21, 2013
Accepted: April 15, 2013
Published: May 13, 2013

REFERENCES

Alizadeh, A.A., Eisen, M.B., Davis, R.E., Ma, C., Lossos, I.S., Rosenwald, A., Boldrick, J.C., Sabet, H., Tran, T., Yu, X., et al. (2000). Distinct types of diffuse large B-cell lymphoma identified by gene expression profiling. Nature *403*, 503–511.

Beard, C., Hochedlinger, K., Plath, K., Wutz, A., and Jaenisch, R. (2006). Efficient method to generate single-copy transgenic mice by site-specific integration in embryonic stem cells. Genesis *44*, 23–28.

Bernstein, B.E., Mikkelsen, T.S., Xie, X., Kamal, M., Huebert, D.J., Cuff, J., Fry, B., Meissner, A., Wernig, M., Plath, K., et al. (2006). A bivalent chromatin structure marks key developmental genes in embryonic stem cells. Cell *125*, 315–326.

Blackman, M.A., Tigges, M.A., Minie, M.E., and Koshland, M.E. (1986). A model system for peptide hormone action in differentiation: interleukin 2 induces a B lymphoma to transcribe the J chain gene. Cell *47*, 609–617.

Cao, R., Wang, L., Wang, H., Xia, L., Erdjument-Bromage, H., Tempst, P., Jones, R.S., and Zhang, Y. (2002). Role of histone H3 lysine 27 methylation in Polycomb-group silencing. Science *298*, 1039–1043.

Casola, S., Cattoretti, G., Uyttersprot, N., Koralov, S.B., Seagal, J., Hao, Z., Waisman, A., Egert, A., Ghitza, D., and Rajewsky, K. (2006). Tracking germinal center B cells expressing germ-line immunoglobulin gamma1 transcripts by conditional gene targeting. Proc. Natl. Acad. Sci. USA *103*, 7396–7401.

Cattoretti, G., Pasqualucci, L., Ballon, G., Tam, W., Nandula, S.V., Shen, Q., Mo, T., Murty, V.V., and Dalla-Favera, R. (2005). Deregulated BCL6 expression recapitulates the pathogenesis of human diffuse large B cell lymphomas in mice. Cancer Cell *7*, 445–455.

Chase, A., and Cross, N.C. (2011). Aberrations of EZH2 in cancer. Clinical cancer research: an official journal of the American Association for Cancer Research *17*, 2613–2618.

Ci, W., Polo, J.M., and Melnick, A. (2008). B-cell lymphoma 6 and the molecular pathogenesis of diffuse large B-cell lymphoma. Curr. Opin. Hematol. *15*, 381–390.

as plasmablasts, are believed to give rise to ABC-DLBCLs. However, the occurrence of EZH2 somatic mutations aberrantly sustains repression of proliferation checkpoint and differentiation genes, resulting in GC hyperplasia, and the presence of other oncogenic hits, such as BCL2, enables transformation to GCB-type DLBCL or FL. A possible alternative route leading to GCB-DLBCL could involve overexpression or aberrant maintenance of WT EZH2 expression. GCB-DLBCLs and FLs but not ABC-DLBCLs require EZH2 to maintain their proliferation and survival. Thus, EZH2 methyltransferase inhibitors suppress GCB-DLBCLs but not ABC-DLBCLs.
See also Figure S7.

Czermin, B., Melfi, R., McCabe, D., Seitz, V., Imhof, A., and Pirrotta, V. (2002). Drosophila enhancer of Zeste/ESC complexes have a histone H3 methyltransferase activity that marks chromosomal Polycomb sites. Cell *111*, 185–196.

De, S., Shaknovich, R., Riester, M., Elemento, O., Geng, H., Kormaksson, M., Jiang, Y., Woolcock, B., Johnson, N., Polo, J.M., et al. (2013). Aberration in DNA methylation in B-cell lymphomas has a complex origin and increases with disease severity. PLoS Genet. *9*, e1003137.

Egle, A., Harris, A.W., Bath, M.L., O'Reilly, L., and Cory, S. (2004). VavP-Bcl2 transgenic mice develop follicular lymphoma preceded by germinal center hyperplasia. Blood *103*, 2276–2283.

Giannopoulou, E.G., and Elemento, O. (2011). An integrated ChIP-seq analysis platform with customizable workflows. BMC Bioinformatics *12*, 277.

Klein, U., and Dalla-Favera, R. (2008). Germinal centres: role in B-cell physiology and malignancy. Nat. Rev. Immunol. *8*, 22–33.

Knutson, S.K., Wigle, T.J., Warholic, N.M., Sneeringer, C.J., Allain, C.J., Klaus, C.R., Sacks, J.D., Raimondi, A., Majer, C.R., Song, J., et al. (2012). A selective inhibitor of EZH2 blocks H3K27 methylation and kills mutant lymphoma cells. Nat. Chem. Biol. *8*, 890–896.

Lohr, J.G., Stojanov, P., Lawrence, M.S., Auclair, D., Chapuy, B., Sougnez, C., Cruz-Gordillo, P., Knoechel, B., Asmann, Y.W., Slager, S.L., et al. (2012). Discovery and prioritization of somatic mutations in diffuse large B-cell lymphoma (DLBCL) by whole-exome sequencing. Proc. Natl. Acad. Sci. USA *109*, 3879–3884.

Mahmoudi, T., and Verrijzer, C.P. (2001). Chromatin silencing and activation by Polycomb and trithorax group proteins. Oncogene *20*, 3055–3066.

McCabe, M.T., Graves, A.P., Ganji, G., Diaz, E., Halsey, W.S., Jiang, Y., Smitheman, K.N., Ott, H.M., Pappalardi, M.B., Allen, K.E., et al. (2012a). Mutation of A677 in histone methyltransferase EZH2 in human B-cell lymphoma promotes hypertrimethylation of histone H3 on lysine 27 (H3K27). Proc. Natl. Acad. Sci. USA *109*, 2989–2994.

McCabe, M.T., Ott, H.M., Ganji, G., Korenchuk, S., Thompson, C., Van Aller, G.S., Liu, Y., Graves, A.P., Della Pietra, A., 3rd, Diaz, E., et al. (2012b). EZH2 inhibition as a therapeutic strategy for lymphoma with EZH2-activating mutations. Nature *492*, 108–112.

Morin, R.D., Johnson, N.A., Severson, T.M., Mungall, A.J., An, J., Goya, R., Paul, J.E., Boyle, M., Woolcock, B.W., Kuchenbauer, F., et al. (2010). Somatic mutations altering EZH2 (Tyr641) in follicular and diffuse large B-cell lymphomas of germinal-center origin. Nat. Genet. *42*, 181–185.

Morin, R.D., Mendez-Lago, M., Mungall, A.J., Goya, R., Mungall, K.L., Corbett, R.D., Johnson, N.A., Severson, T.M., Chiu, R., Field, M., et al. (2011). Frequent mutation of histone-modifying genes in non-Hodgkin lymphoma. Nature *476*, 298–303.

Mortazavi, A., Williams, B.A., McCue, K., Schaeffer, L., and Wold, B. (2008). Mapping and quantifying mammalian transcriptomes by RNA-Seq. Nat. Methods *5*, 621–628.

Müller, J., Hart, C.M., Francis, N.J., Vargas, M.L., Sengupta, A., Wild, B., Miller, E.L., O'Connor, M.B., Kingston, R.E., and Simon, J.A. (2002). Histone methyltransferase activity of a Drosophila Polycomb group repressor complex. Cell *111*, 197–208.

O'Carroll, D., Erhardt, S., Pagani, M., Barton, S.C., Surani, M.A., and Jenuwein, T. (2001). The polycomb-group gene Ezh2 is required for early mouse development. Mol. Cell. Biol. *21*, 4330–4336.

Qi, W., Chan, H., Teng, L., Li, L., Chuai, S., Zhang, R., Zeng, J., Li, M., Fan, H., Lin, Y., et al. (2012). Selective inhibition of Ezh2 by a small molecule inhibitor blocks tumor cells proliferation. Proc. Natl. Acad. Sci. USA *109*, 21360–21365.

Raaphorst, F.M., van Kemenade, F.J., Fieret, E., Hamer, K.M., Satijn, D.P., Otte, A.P., and Meijer, C.J. (2000). Cutting edge: polycomb gene expression patterns reflect distinct B cell differentiation stages in human germinal centers. J. Immunol. *164*, 1–4.

Rui, L., Schmitz, R., Ceribelli, M., and Staudt, L.M. (2011). Malignant pirates of the immune system. Nat. Immunol. *12*, 933–940.

Shih, A.H., Abdel-Wahab, O., Patel, J.P., and Levine, R.L. (2012). The role of mutations in epigenetic regulators in myeloid malignancies. Nat. Rev. Cancer *12*, 599–612.

Shin, D.M., Liu, R., Wu, W., Waigel, S.J., Zacharias, W., Ratajczak, M.Z., and Kucia, M. (2012). Global gene expression analysis of very small embryonic-like stem cells reveals that the Ezh2-dependent bivalent domain mechanism contributes to their pluripotent state. Stem Cells Dev. *21*, 1639–1652.

Sneeringer, C.J., Scott, M.P., Kuntz, K.W., Knutson, S.K., Pollock, R.M., Richon, V.M., and Copeland, R.A. (2010). Coordinated activities of wild-type plus mutant EZH2 drive tumor-associated hypertrimethylation of lysine 27 on histone H3 (H3K27) in human B-cell lymphomas. Proc. Natl. Acad. Sci. USA *107*, 20980–20985.

Su, I.H., Basavaraj, A., Krutchinsky, A.N., Hobert, O., Ullrich, A., Chait, B.T., and Tarakhovsky, A. (2003). Ezh2 controls B cell development through histone H3 methylation and Igh rearrangement. Nat. Immunol. *4*, 124–131.

Taniguchi, H., Jacinto, F.V., Villanueva, A., Fernandez, A.F., Yamamoto, H., Carmona, F.J., Puertas, S., Marquez, V.E., Shinomura, Y., Imai, K., and Esteller, M. (2012). Silencing of Kruppel-like factor 2 by the histone methyltransferase EZH2 in human cancer. Oncogene *31*, 1988–1994.

Trapnell, C., Pachter, L., and Salzberg, S.L. (2009). TopHat: discovering splice junctions with RNA-Seq. Bioinformatics *25*, 1105–1111.

van Galen, J.C., Dukers, D.F., Giroth, C., Sewalt, R.G., Otte, A.P., Meijer, C.J., and Raaphorst, F.M. (2004). Distinct expression patterns of polycomb oncoproteins and their binding partners during the germinal center reaction. Eur. J. Immunol. *34*, 1870–1881.

van Kemenade, F.J., Raaphorst, F.M., Blokzijl, T., Fieret, E., Hamer, K.M., Satijn, D.P., Otte, A.P., and Meijer, C.J. (2001). Coexpression of BMI-1 and EZH2 polycomb-group proteins is associated with cycling cells and degree of malignancy in B-cell non-Hodgkin lymphoma. Blood *97*, 3896–3901.

Velichutina, I., Shaknovich, R., Geng, H., Johnson, N.A., Gascoyne, R.D., Melnick, A.M., and Elemento, O. (2010). EZH2-mediated epigenetic silencing in germinal center B cells contributes to proliferation and lymphomagenesis. Blood *116*, 5247–5255.

Verma, S.K., Tian, X., LaFrance, L.V., Duquenne, C., Suarez, D.P., Newlander, K.A., Romeril, S.P., Burgess, J.L., Grant, S.W., Brackley, J.A., et al. (2012). Identification of potent, selective, cell-active inhibitors of the histone lysine methyltransferase EZH2. ACS Med. Chem. Lett. *3*, 1091–1096.

Yap, D.B., Chu, J., Berg, T., Schapira, M., Cheng, S.W., Moradian, A., Morin, R.D., Mungall, A.J., Meissner, B., Boyle, M., et al. (2011). Somatic mutations at EZH2 Y641 act dominantly through a mechanism of selectively altered PRC2 catalytic activity, to increase H3K27 trimethylation. Blood *117*, 2451–2459.

Yu, J., Cao, Q., Mehra, R., Laxman, B., Yu, J., Tomlins, S.A., Creighton, C.J., Dhanasekaran, S.M., Shen, R., Chen, G., et al. (2007). Integrative genomics analysis reveals silencing of beta-adrenergic signaling by polycomb in prostate cancer. Cancer Cell *12*, 419–431.